Available online at www.sciencedirect.com
ScienceDirect
International Journal of Pharmaceutics 337 (2007) 40–47
INTERNATIONAL JOURNAL OF PHARMACEUTICS
www.elsevier.com/locate/ijpharm

Adsorption of bovine serum albumin (BSA) onto lecithin studied by attenuated total reflectance Fourier transform infrared (ATR-FTIR) spectroscopy

R. Tantipolphan [a], T. Rades [a], A.J. McQuillan [b], N.J. Medlicott [a,*]

[a] *School of Pharmacy, The University of Otago, Dunedin, New Zealand*
[b] *Chemistry Department, The University of Otago, Dunedin, New Zealand*

Received 12 September 2006; received in revised form 18 December 2006; accepted 18 December 2006
Available online 23 December 2006

Abstract

The adsorption of bovine serum albumin (BSA) to lecithin was investigated by ATR-FTIR spectroscopy. Lecithin films were prepared by casting aliquots of 3.2 μg lecithin in methanol onto ZnSe ATR prisms. Surface morphology and the thickness of the films were investigated by laser scanning confocal electron microscopy and scanning electron microscopy and the thickness of the films used for adsorption studies was estimated to be 40 Å. The dependency of the C=O peak area on the lecithin mass in the calibration curve confirms that the thickness of the film is below the penetration depth of the infrared evanescent wave. Size exclusion HPLC and fluorescence spectroscopy show that BSA conformation in up to 1 M NaCl and $CaCl_2$ solutions is similar to that in water with no aggregation or changes in protein conformation seen over 4 h. The kinetics of BSA adsorption on the lecithin film from water, NaCl and $CaCl_2$ solutions demonstrates that ions promote the protein adsorption. BSA bound more in the presence of NaCl compared to $CaCl_2$ at equivalent concentrations. The adsorption appeared greatest at a 0.1 M concentration for both NaCl and $CaCl_2$. The results are explained in terms of absorptive reactivity of BSA and lecithin surfaces upon salt addition.

Keywords: ATR-FTIR; Protein adsorption; Phospholipid; NaCl and $CaCl_2$

1. Introduction

Liposomes as particulate phospholipid dispersions have shown promise as targeted drug delivery systems for cytotoxic agents, vaccine antigens and DNA (Oku et al., 2001; Harrington et al., 2002; Leserman, 2004). Upon hydration, the polar headgroups of phospholipids readily orientate towards the bulk water phase whereas the hydrophobic tail groups associate away from the water (Harrington et al., 2002). Polar headgroup surfaces (external and internal) are therefore available to interact with protein in solution during formulation. When therapeutic agents have higher ordered structures, such as the secondary and tertiary structures of proteins, it is important to study changes in these structures that may occur during their formulation, storage and use and the effects of formulation excipients on these structures so that losses in biological activity can be minimized.

In mixtures that comprise protein, water and phospholipid, many potential interfaces exist throughout the system. Upon adsorption at an interface the native structure of the protein can be disrupted and, subsequently, a loss or decrease in the biological activity may occur (Green et al., 1999; Sethuraman and Belfort, 2005; Mollmann et al., 2006). Additionally, any perturbed proteins which desorb from hydrophobic surfaces can act as precursors to protein aggregation (Norde and Giacomelli, 2000). The severity of conformational alteration depends on the characteristics of protein, surfaces and the environment involved. Binding of horseradish peroxidase (HRP) onto a mica surface is accompanied by a strong protein–protein interaction of the adsorbed proteins and subsequently induced aggregation of the molecules at the interface (Tang et al., 2002). While a modification in the tertiary structure was detected, HRP retained its secondary structure and enzymatic activity upon adsorption onto dimyristoylphosphatidylcholine (DMPC) membranes. Additional to the issues concerning the stability of the bioactive

* Corresponding author at: School of Pharmacy, The University of Otago, P.O. Box 913, Dunedin 9015, New Zealand. Tel.: +64 3 479 7275; fax: +64 3 479 7034.
E-mail address: natalie.medlicott@stonebow.otago.ac.nz (N.J. Medlicott).

0378-5173/$ – see front matter © 2006 Elsevier B.V. All rights reserved.
doi:10.1016/j.ijpharm.2006.12.021

molecules, protein adsorption onto a phospholipid interface may change the surface rheological behaviour from a liquid-like to a gel-like monolayer, increase monolayer surface roughness, and induce flocculation or aggregation of liposomes (Bergers et al., 1993; Dimitrova et al., 1997; Roberts et al., 2005; De Souza et al., 2006). Therefore, the investigation of lipid–protein interactions is necessary to achieve a better understanding of the protein release from lipid based delivery systems.

We hypothesize that the reactivity towards protein adsorption of the phospholipid headgroup surfaces is dependant on hydration and dehydration effects caused by excipients such as salts in the formulation. Attenuated total reflectance Fourier transform infrared (ATR-FTIR) spectroscopy is a technique that can be used to study the association of solute molecules onto fixed surfaces (Hubner and Blume, 1998; Vermette et al., 2003; McClellan and Franses, 2005) and therefore can potentially be used to study adsorption of proteins onto phospholipids. In this paper we describe an application of ATR-FTIR spectroscopy to study adsorption of bovine serum albumin (BSA) onto hydrated lecithin films from aqueous solutions in the presence of sodium chloride and calcium chloride. BSA is a globular protein with an approximate molecular weight 66 kDa. It has been considered as a soft protein, implying that the molecules have a high potential to undergo structural rearrangements upon adsorption onto interfaces (McClellan and Franses, 2005).

2. Materials and methods

2.1. Materials

Freeze dried BSA was purchased from Sigma (Australia) and stored at −20 °C over dried silica. Hydrogenated soybean lecithin (Lipoid S100-3) was purchased from Lipoid (Germany). Sodium chloride was obtained from Merck (Germany). Calcium chloride dihydrate was from Fluka (Australia). All other chemicals were analytical grade purchased from BDH Chemicals (England).

2.2. ATR-FTIR measurements

ATR-FTIR interferograms were acquired using a BioRad FTS 175C FTIR spectrometer fitted with a ZnSe multiple reflection prism (Pike technologies, trough plate) with a fixed incident angle of 45°, 10 reflections, and an area of 4.32 cm^2. A flow cell fabricated to allow liquids to be passed over the ZnSe surface was fitted and connected to a peristaltic pump (ISCO Tris). A flow rate of 2.0 ml/min was used in all experiments. To minimize the effects of water vapor on the IR spectra, the chamber containing the ATR cell was continuously purged with dry air. Single beam spectra were collected from 16 scans at a resolution of 4 cm^{-1} and the data was manipulated using GRAMS/AI 7.01 (Galactic Industries Corp.).

2.3. Characterization of the lecithin film by ATR-FTIR

Prior to the experiment, the ZnSe surface was polished with a slurry of aluminium oxide (particle size 0.015 μm) in water and then washed with water and methanol. Lecithin films were prepared by casting 200 μl of 0.0008–0.1% (w/v) lecithin in methanol (equivalent to 1.6–200 μg lecithin mass) onto the ZnSe prism. The methanol was evaporated over an hour in a dessicator with dried silica gel followed by a water pump vacuum for 10 min at room temperature. The absorbance spectra of lecithin films from increasing concentrations ($n = 10$ for 0.0016%, w/v lecithin and $n = 3$ for the other concentrations) were obtained using the blank ZnSe as the background.

2.4. Adsorption studies

Films cast from 3.2 μg lecithin were hydrated by passing aqueous solutions containing 0, 0.1 and 1.0 M NaCl or $CaCl_2$ over the surface for 60 min at room temperature. Then the solution was replaced with 0.01% (w/v) BSA in the corresponding salt solutions and recirculated for a further 60 min ($n = 3$–4). All of the solutions were filtered (0.45 μm membrane) prior to use. Deposition of BSA on the hydrated lecithin films was determined by converting the interferograms after BSA was added to the circulating solutions to absorbance spectra using the interferogram of hydrated lecithin at 60 min as the background. The kinetics of BSA adsorption onto lecithin was monitored by determining the increase in the integrated amide II peak area (1600–1480 cm^{-1}) over time.

2.5. Image analyses

To investigate the film properties, lecithin films were cast from aliquots of 200 μg lecithin in methanol onto glass microscopy slides having the same surface area as the ZnSe prism used in the ATR study ($n = 2$). The surface morphology was investigated using laser scanning confocal electron microscopy (LSCM) in the reflectance scanning mode (Zeiss 510 LSM confocal with Axioplan 2 upright microscope). To determine the film thickness, the glass slide was cracked through the lecithin film. The cross-sectional surface was sputter coated with 5 nm gold palladium (Emitech K575X) and viewed by scanning electron microscopy (JEOL 6700F field emission SEM). The film thickness was obtained by measuring the distance between the film and glass surface. The reported value is the average obtained from three measurement from two independent cuts in each film.

2.6. Size exclusion HPLC (SE-HPLC)

SE-HPLC was used to monitor aggregation of 0.01% (w/v) BSA in 0, 0.1, 1, 3 and 5 M NaCl solutions. Solutions were incubated in a 25 °C shaking (60 rpm) water bath for 0, 0.5, 1, and 4 h ($n = 2$). Analysis was performed using a BioSep-SEC-S2000 column (5 μm hydrophilic bonded silica, 300 mm × 7.8 mm from Phenomenex). The mobile phase comprised 10 mM sodium phosphate buffer, 100 mM NaCl, pH 7.0 with a flow rate of 0.8 ml/min. The injection volume was 100 μl. Chromatograms were acquired using a UV absorption detector at 220 and 280 nm and a fluorescence detector with an excitation wavelength of 297 nm and emission at 338 nm.

2.7. Fluorescence spectroscopy

Changes in the intrinsic fluorescence intensity and maximum wavelength in the fluorescence emission spectra were used to investigate conformational perturbation of BSA in salt solutions (0, 0.1, 1, 3 and 5 M NaCl and $CaCl_2$). The samples were excited at 297 nm and the emission spectra were recorded from 300 to 400 nm using a Shimadzu RF540 spectrofluorometer at room temperature. The excitation and emission monochromator bandwidths were 5 nm. One-way ANOVA was used to test the differences in the emission intensities and was performed using Minitab Release 14.12.0 (Minitab Inc.).

3. Results

3.1. ATR-FTIR spectra and morphology of lecithin films

Fig. 1 shows a typical absorbance spectrum of a lecithin film cast on the ZnSe prism. The most prominent features are bands corresponding to the hydrophobic tail regions at 2850, 2917, 2956, and 1468 cm^{-1}. These represent symmetric CH_2 ($\upsilon_s CH_2$), antisymmetric CH_2 ($\upsilon_{as} CH_2$), antisymmetric CH_3 ($\upsilon_{as} CH_3$) stretching and CH_2 scissoring, respectively (Mantsch and McElhaney, 1991; Tamm and Tatulian, 1997; McClellan and Franses, 2005). The peak at 1737 cm^{-1} represents the C=O stretching. This group is located between hydrophobic tails and hydrophilic head group of the lecithin molecule. The peak at 1168 cm^{-1} is assigned to asymmetric CO–O–C stretching. The $N^+(CH_3)_3$ stretching is located at 972 cm^{-1}. Peaks at 1240 and 1092 cm^{-1} arise from the vibrations of antisymmetric (υ_{as}) and symmetric (υ_s) PO_2^- stretching.

Films deposited on the ZnSe were characterized by monitoring the C=O stretching. The integrated C=O peak area (1770–1700 cm^{-1}) of the films cast from 1.6 to 200 μg lecithin in methanol were used to prepare a calibration curve. Fig. 2 shows that the peak area increases linearly upon increasing the concentration of lecithin in methanol solution ($R^2 > 0.99$). To minimize the variability of the film surface from sample to sample, lecithin films prepared from 3.2 μg (or 0.0016%, w/v) lecithin in methanol solution having the integrated peak area between 0.18 and 0.13 cm^{-1} were used for adsorption studies.

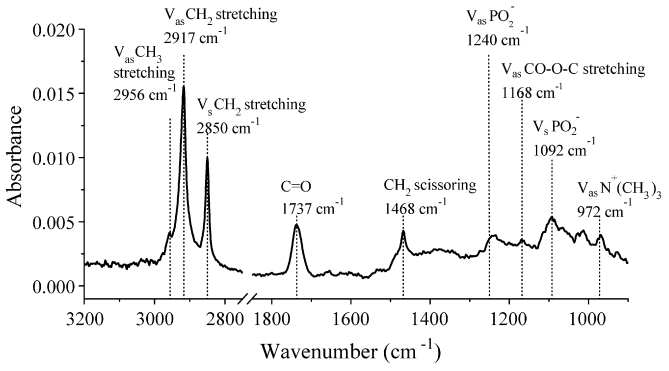

Fig. 1. ATR spectrum of a lecithin film cast on a ZnSe multireflectance prism (surface area = 4.32 cm^2) from 3.2 μg lecithin in methanol.

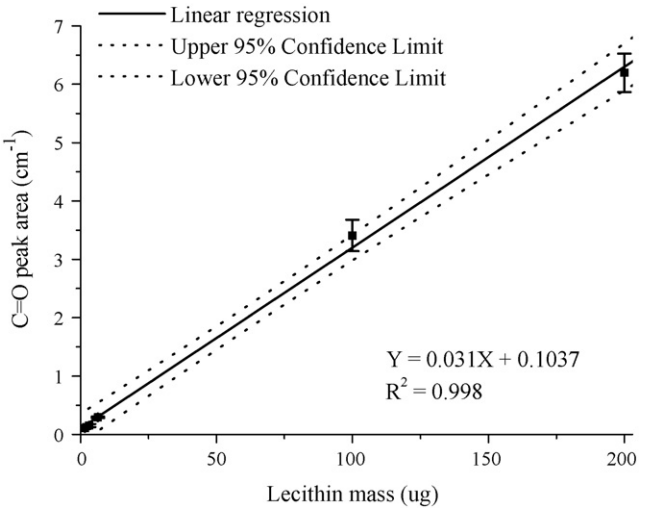

Fig. 2. Calibration curve prepared from integrated C=O peak area (1770–1700 cm^{-1}) of lecithin films cast on ZnSe prism from 1.6 to 200 μg lecithin in methanol.

Film thickness and morphology were studied from the films cast from 200 μg lecithin in methanol and inference about the physical form of the thinner films had to be made from these results due to the resolution limitation of the imaging techniques used in this study. The reflectance image from LSCM shows that lecithin films exhibited a rough surface (Fig. 3a). When the glass slides were cracked and the transverse section though

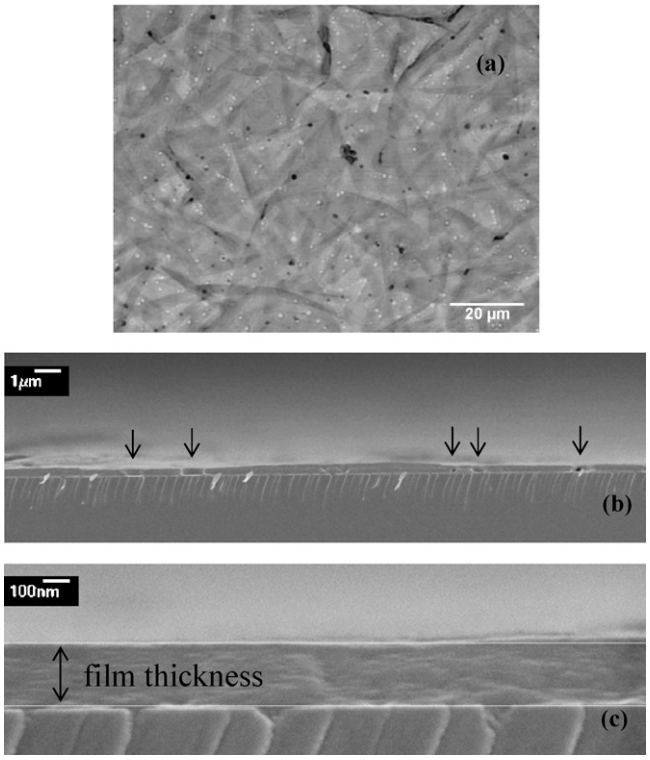

Fig. 3. (a) LSCM image from a reflectance scan of the lecithin film. SEM images of lecithin film at (b) 5000× and (c) 50,000× magnifications. The arrows in (b) show defects in the film. Films were prepared by deposition of 200 μg lecithin.

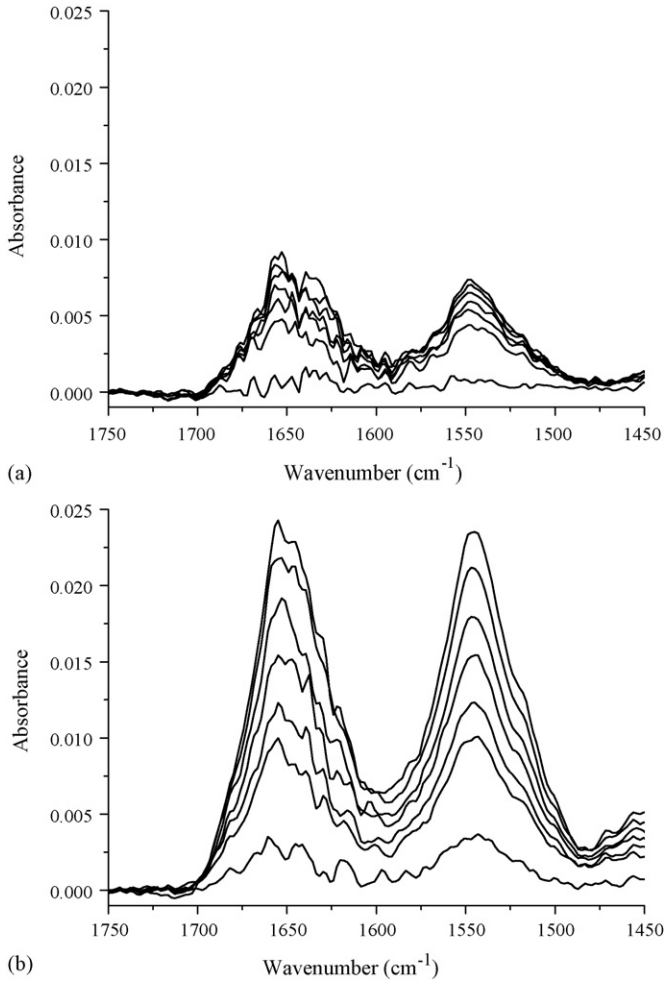

Fig. 4. ATR-FTIR absorbance spectra showing increased deposition of BSA from 0.01% (w/v) BSA in (a) water and (b) 0.1 M NaCl solution onto lecithin over 60 min. From the bottom to the top spectra, the single beam interferograms taken at 1, 10, 20, 30, 40, 50, and 60 min were converted to ATR spectra using the single beam interferogram taken after the film was hydrated with salt solutions for 60 min as a background.

the film examined using SEM (Fig. 3b), the image did confirm the existence of some imperfections as marked by the arrows in Fig. 3b. Closer examination of the imperfections suggested these were small holes of less than 0.5 μm diameter. The average thickness of the films was estimated to be 260 ± 38 nm (Fig. 3c). Using this information and the mass of the lecithin, the thickness of the film cast from the 3.2 μg lecithin was estimated to be approximately 40 Å.

3.2. Kinetics of BSA adsorption onto the lecithin surface

A progressive growth of the amide bands was seen when solutions of 0.01% (w/v) BSA were passed over lecithin on ZnSe. Fig. 4a and b show the amide band appearance from water and 0.1 M NaCl solutions, respectively. The amide I peak centered at 1655 cm^{-1} and the amide II band at 1545 cm^{-1}, which is consistent with published band positions (McClellan and Franses, 2005; Sethuraman and Belfort, 2005). The amide

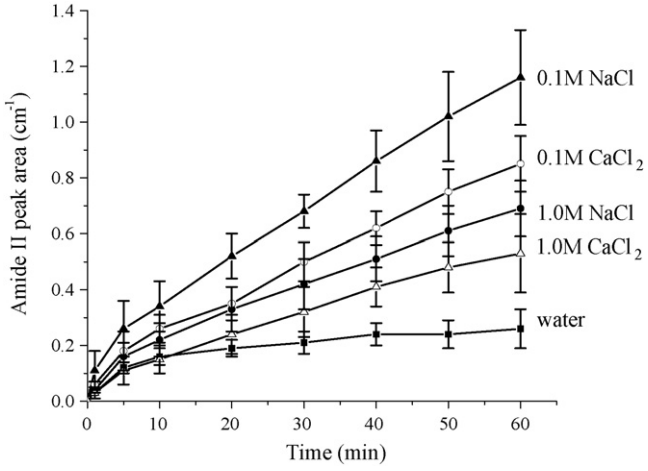

Fig. 5. Kinetics of BSA deposition from aqueous salt solutions onto hydrated lecithin films.

II band is reported to be less conformational sensitive than the amide I band and has been used for quantitative analysis of protein deposition onto various interfaces (Fu et al., 1993; Vermette et al., 2003). Using the peak area of the amide II band the kinetics of deposition of BSA onto lecithin film was determined (Fig. 5). These results indicate that salts (NaCl and $CaCl_2$) promote the adsorption of BSA onto lecithin surfaces. Without salts, BSA adsorption was the lowest and an equilibrium was reached after about 40 min. From NaCl and $CaCl_2$ solutions, more BSA was adsorbed and equilibrium was not reached within the 60 min experiment. Interestingly, BSA deposition appeared greatest at the lower salt concentration (0.1 M) for both NaCl and $CaCl_2$. Furthermore BSA adsorption from NaCl solutions appeared higher than from $CaCl_2$ solutions for both 0.1 and 1 M concentrations.

3.3. SE-HPLC of BSA in NaCl solutions

SE-HPLC is a commonly used technique to investigate protein aggregation (Wang, 1999). Fig. 6 shows typical size exclusion chromatograms of BSA consisting of dimer and monomer peaks at 8.2 and 9.1 min, respectively. The absence of peaks prior to the dimer peak upon addition of up to 3 M NaCl indicates that BSA did not aggregate in the solutions. The chromatograms obtained when up to 3 M NaCl was added appeared similar to that in water suggesting that BSA has a similar molecular shape in these solutions. Changes in the chromatogram seen in 5 M NaCl solution included a broadening of the monomer peak, a shift of the peak retention time to approximately 9.6 min and an appearance of a shoulder at 9.1 min. Upon incubation at 25 °C for 4 h, the chromatograms in 0–3 M NaCl samples appeared unchanged (Fig. 6b). In 5 M NaCl, a progressive broadening and shift in the retention time of the monomer peak to approximately 9.7 min was observed along with an increase in the peak shoulder. A summary of the retention times from each sample is given in Table 1. Similar results were obtained for UV detection at 280 nm and fluorescence detection (data not shown).

Table 1
Retention times of the BSA dimer (top) and monomer (bottom) peaks in size exclusion chromatograms

Incubation time (h)	NaCl concentration (M)				
	0	0.1	1	3	5
0	8.24 ± 0.03 9.06 ± 0.06	8.23 ± 0.02 9.05 ± 0.03	8.25 ± 0.02 9.07 ± 0.04	8.25 ± 0.01 9.10 ± 0.01	8.30 ± 0.02 9.61 ± 0.05
0.5	8.25 ± 0.01 9.08 ± 0.01	8.28 ± 0.05 9.11 ± 0.04	8.29 ± 0.02 9.11 ± 0.01	8.28 ± 0.01 9.13 ± 0.01	8.32 ± 0.03 9.64 ± 0.01
1	8.28 ± 0.04 9.10 ± 0.04	8.27 ± 0.01 9.10 ± 0.01	8.28 ± 0.02 9.12 ± 0.02	8.26 ± 0.05 9.11 ± 0.04	8.33 ± 0.04 9.67 ± 0.02
4	8.22 ± 0.05 9.04 ± 0.05	8.28 ± 0.01 9.10 ± 0.01	8.28 ± 0.00 9.11 ± 0.01	8.31 ± 0.02 9.15 ± 0.02	8.32 ± 0.01 9.71 ± 0.09

3.4. Fluorescence spectroscopy of BSA in NaCl and $CaCl_2$ solutions

Changes in the fluorescence emission intensity at 338 nm and the maximum wavelength (λ_{max}) in the emission spectra on incubation of BSA in NaCl and $CaCl_2$ solutions are shown in Fig. 7a and b, respectively. A shift in the intensity and λ_{max} reflects changes in the protein conformation. Intensity decreased slightly in 3 and 5 M NaCl solutions and dropped sharply in 3 and 5 M $CaCl_2$ solutions (Fig. 7a). At the same time, the λ_{max} in the fluorescence emission spectra shifted slightly from 344 nm in aqueous solution to 342 nm for 5 M NaCl and to 331 nm for 3 and 5 M $CaCl_2$ solutions (Fig. 7b). These results suggest that the conformation of BSA in 3 and 5 M $CaCl_2$ and NaCl solutions differ from that of aqueous solution. No further changes in the fluorescence intensity and λ_{max} were observed after incubation at 25 °C for 4 h.

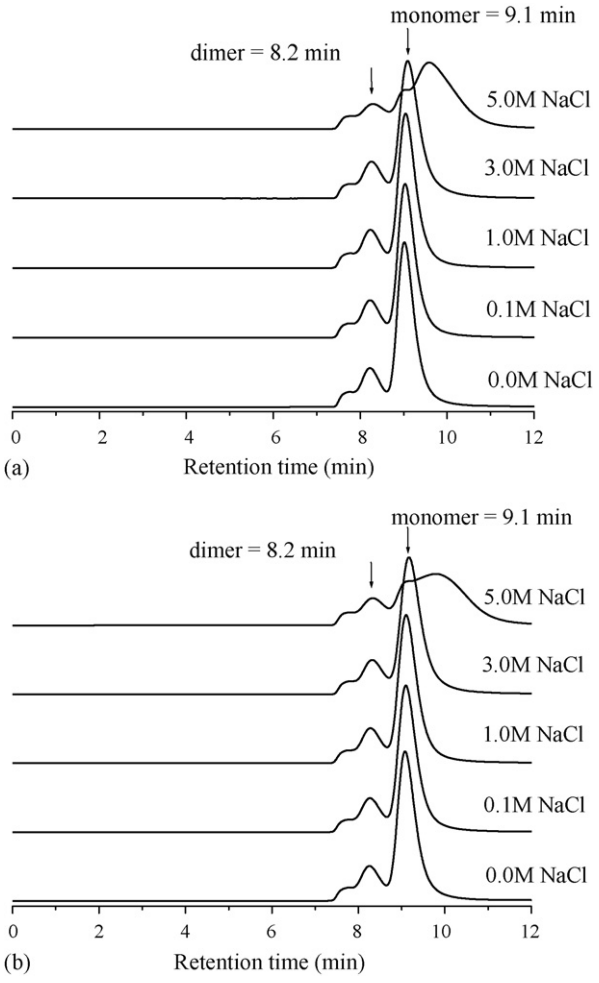

Fig. 6. Typical size exclusion chromatograms of BSA in NaCl solutions using a UV detector at 220 nm. The chromatograms were obtained after the samples were incubated at 25 °C for (a) 0 h and (b) 4 h.

4. Discussion

ATR-FTIR is becoming a valuable technique in the investigation of protein adsorption onto phospholipids (Vermette et al., 2003; McClellan and Franses, 2005). Fig. 8 illustrates a schematic drawing of the ATR experimental setup used in this study. An evanescent wave is generated at the point of total internal reflectance of the IR beam which penetrates into the sample deposited on the surface of the ZnSe prism. This allows information on the molecular composition of materials on the ZnSe surface to be obtained. The depth of penetration of the evanescent wave depends on the refractive index of the medium in contact with the ZnSe surface and the infrared wavelength (Mirabella, 1998). For an aqueous salt solution having the refractive index of 1.5 circulating on the ZnSe prism, the penetration depth at mid-IR ranges from 0.5 to 3 μm. In our work, by ensuring the lecithin film is thin enough for the evanescent wave to penetrate through to the interface between the film and an overlying aqueous phase it was possible to study the adsorption of compounds from the bulk solution phase to the interface. Further, to investigate the possible driving force(s) for protein adsorption at the phospholipid-aqueous interface three areas of interest were identified and investigated. These were (i) the deposited lecithin film, (ii) the interface and (iii) the bulk solution phases (Fig. 8).

In accordance with previous publications, the ATR spectra of thin film casts from 3.2 μg lecithin in methanol contained peaks corresponding to hydrophobic tail groups (C–H stretching) and hydrophilic headgroup (phosphate vibration) of the phospholipid linked via a glycerol residue as shown in Fig. 1 (Mantsch and McElhaney, 1991; McClellan and Franses, 2005). The linear relationship observed between the peak areas of the C=O

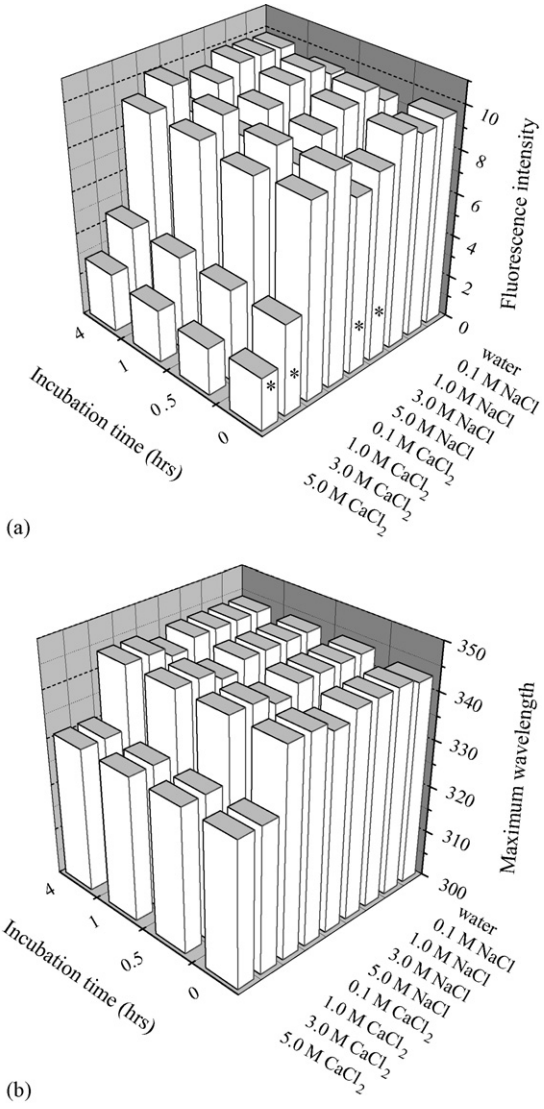

Fig. 7. A summary of (a) the intrinsic fluorescence emission intensity at 338 nm and (b) the λ_{max} in the emission spectra of BSA. The excitation wavelength = 297 nm. At 0 h, the asterisks indicate statistical differences in the intensity compared to the intensity from aqueous solution using one-way ANOVA.

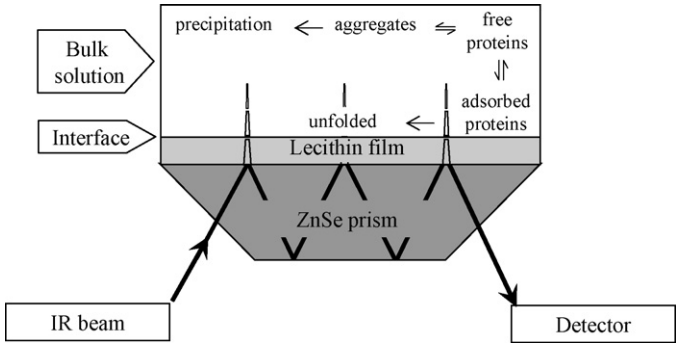

Fig. 8. Diagrammatic presentation of the ATR experiment, showing total internal reflectance of the IR laser beam and generation of evanescent waves that penetrate through the sample deposited on the surface of the ZnSe prism.

vibration and lecithin mass ($R^2 > 0.99$, Fig. 2) suggests that the evanescent IR wave penetrates through the deposited film and this peak was used to quantify the film thickness of films prepared from up to 200 μg lecithin. LSCM and SEM images were acquired for films prepared from 200 μg lecithin to characterize the surface morphology and film thickness, respectively as the thinner films could not be visualized by microscopy (Fig. 3). The images reveal that the surface of the film is rough containing of cracks and holes throughout the layer. The thickness of the film cast from 200 μg lecithin was 260 ± 38 nm. Therefore, we estimated the lecithin film thickness in the adsorption studies where the mass of lecithin deposited was 3.2 μg lecithin to be approximately 40 Å. This thickness is slightly smaller than the reported thickness of lecithin bilayers (Small, 1986; Tang et al., 2002). Hence, it is likely that the phospholipid surface consists of a mixture of mono and bilayers, and possibly a small proportion of multilayers.

At the interface the spectral contribution from the protein in bulk solution was minimized by using a low protein concentration (0.01%, w/v) in the bulk circulating solution. The ATR spectra in the absence of a lecithin layer show insignificant amide I and II bands at this concentration if no accumulation on the ZnSe occurs (data not shown). On recirculating the BSA solutions over hydrated lecithin films progressive increase in the amide I and II bands over time was seen indicating increased deposition of BSA onto the lecithin surface. The amide I band for proteins yields information about secondary structure (Green et al., 1999; McClellan and Franses, 2005; Sethuraman and Belfort, 2005) but overlapping bands from bulk water in these studies resulted in a noisy amide I band so the protein secondary structure could not be determined (Fig. 4). The amide II band is not significantly affected by bulk water (Fu et al., 1993; Vermette et al., 2003) and thus was used to quantify the BSA adsorption. The kinetics of BSA adsorption from salt solutions onto lecithin films was determined by monitoring increases in the amide II peak area over time and showed that the amount of adsorbed BSA increased in the following order: 0.1 M NaCl > 0.1 M $CaCl_2$ > 1.0 M NaCl > 1.0 M $CaCl_2$ > water (Fig. 5). Therefore, using ATR it was possible to identify differential effects of salts and salt concentrations on adsorption of a protein onto a phospholipid surface. Potentially this technique also lends itself to studying the effects of many other formulation excipients on protein adsorption in lipid formulations. From the adsorption studies reported in this paper it can be concluded that:

- BSA adsorption was promoted by salts (either NaCl or $CaCl_2$);
- BSA adsorption at equivalent concentrations (0.1 or 1.0 M) was greater from NaCl solutions than $CaCl_2$ solutions;
- BSA adsorption was greatest for either salt (NaCl or $CaCl_2$) at the lower concentration.

Protein adsorption involves a wide range of surface and interfacial phenomena (Bergers et al., 1993; Green et al., 1999; Roberts et al., 2005). The most important driving forces for the adsorption appear to be electrostatic and hydrophobic inter-

actions. The relative significance of these interactions in any given system depends on the concentration and physicochemical properties of proteins such as charge and conformation and the characteristics of the surface involved. In addition to direct binding of ions onto protein and phospholipid surfaces, the properties of the water surrounding molecules in solution are influenced by ions. Our observation that ions enhance the adsorption of proteins onto lecithin surfaces may result from an increase in the polarity of the aqueous phase upon salt addition. Therefore, the proteins tend to escape from this environment by adsorbing to the lecithin film, i.e., salting-out onto the lecithin film. According to the Hofmeister series (Cacace et al., 1997; Wang, 1999), Ca^{2+} is more destabilizing towards proteins than Na^{+}, therefore at an equivalent molar concentration, we would expect greater deposition (salting-out) of BSA from the $CaCl_2$ solutions. However, this was not observed in our work so other explanations were sought.

Ca^{2+} has been reported to have a higher affinity than Na^{+} for both protein (Arakawa and Timasheff, 1984) and phospholipids (Kwon et al., 1994; Hubner and Blume, 1998; Binder and Zschornig, 2002). Therefore, the less favourable adsorption of BSA from $CaCl_2$ solutions onto lecithin surfaces (Fig. 5) may have occurred because either greater protein modification (e.g., denaturation or aggregation) occurred in the bulk solution or Ca^{2+} caused a greater modification to the phospholipid surface on binding.

Binding of Ca^{2+} to the phospholipid headgroup has been shown to induce changes in the carbonyl and phosphate vibrations corresponding to headgroup reorientation and lead to the dehydration of phospholipid headgroup by displacement of the water molecules (Kwon et al., 1994; Binder and Zschornig, 2002). An accumulation of Ca^{2+} ions at phospholipid and protein surfaces may generate positive charge at the interface leading to increased electrostatic repulsion, and subsequently resulting in a reduced deposition of BSA onto the lecithin surface in $CaCl_2$ solution. Salt binding effects have been shown to increase upon increasing salt concentrations. The smaller amount of BSA adsorbed from high salt solutions (NaCl and $CaCl_2$) suggests a modified surface charge by ion adsorption contributes to reducing protein adsorption at higher salt concentrations. As mentioned above Ca^{2+} binds more strongly to phospholipid headgroups than Na^{+} so at equivalent concentrations BSA absorption should be less from $CaCl_2$ than NaCl which is consistent with our results.

In the bulk solution phase, ions can affect protein conformation and solubility via preferential hydration and ion binding mechanisms (Chen, 1992; Wang, 1999). As salt concentrations increase, protein–protein interactions favouring attraction and eventually aggregation can occur. This effect may also contribute to the reduction in BSA adsorption to lecithin as salt concentration increased for both NaCl and $CaCl_2$. From the SE-HPLC analysis, it was clear that BSA did not aggregate upon incubation for 4 h in solutions with up to 3 M NaCl (Fig. 6). At 5 M NaCl, BSA chromatograms showed a broadening of the peak shape with increasing retention times suggesting that the molecules in high salt solution adopt a more compact structure compared to the native conformation or they interact by an adsorption mechanism with the HPLC stationary phase. Protein conformation in $CaCl_2$ solutions was not investigated by SE-HPLC because the presence of phosphate ions in the mobile phase produced a risk of $CaPO_4$ precipitation during analysis. Further investigation of BSA conformation in the presence of NaCl and $CaCl_2$ was performed by fluorescence spectroscopy.

The decrease in the fluorescence intensity (Fig. 7a) and the blue-shift of the λ_{max} (Fig. 7b) implies that BSA undergoes structural modification in 3 and 5 M NaCl and $CaCl_2$ solutions. Heat-induced inactivation of BSA decreases the intrinsic fluorescence emission intensity and shifts the λ_{max} from 342 to 334 nm indicating a reduced accessibility of solvent to the tryptophan residues in the denatured state (Tani et al., 1995). However, BSA unfolding induced by 6 M guanidinium hydrochloride corresponds to a shift of the λ_{max} to 352 nm followed by a greater decrease in the intensity compared to the heat treatment (Tani et al., 1995). Our results suggest that the BSA conformation in up to 1 M NaCl and $CaCl_2$ solutions are similar to that in water. Salt denaturation (3 and 5 M NaCl and $CaCl_2$) may generate an intermediate structure that resembles the heat treatment in which the molecules apparently adopt a more compact conformation. This conclusion is supported by the SE-HPLC results that the monomer peak required a longer time to elute implying a more tightly packed structure in high salt solutions. Therefore, the reduced adsorption of BSA from 1 M salt (NaCl and $CaCl_2$) solutions in our study is unlikely to be the consequence of reduced BSA availability for adsorption since the structural alterations of BSA in the bulk solution phase were not observed until salt concentrations of $\geq$3 M.

5. Conclusions

ATR-FTIR spectroscopy was used to investigate the adsorption of BSA onto lecithin films. This technique may be applicable for studying many of the surface adsorption events that occur in protein containing lipid formulations. Our results with two salts suggested salt-type (NaCl and $CaCl_2$) and concentration were important in modifying BSA adsorption to phospholipid. The most likely explanation of the increased adsorption of BSA in the presence of low concentrations of salts is a salting-out of the protein onto the phospholipid. At higher concentrations, or in the presence of salts (Ca^{2+}) with a higher affinity for the phospholipid, ion-binding of the salt to the phospholipid reduces the interaction of protein from solution with the lecithin films.

Acknowledgements

This work was carried out with financial support from a University of Otago Research Grant. We would also like to thank Andrew McNaughton and Liz Girvan for their assistance and advice on LSCM and SEM.

References

Arakawa, T., Timasheff, S.N., 1984. Preferential interactions of proteins with salts in concentrated solutions. Biochemistry 21, 6545–6552.

Bergers, J.J., Vingerhoeds, M.H., Van Bloois, L., Herron, J.N., Janssen, L.H., Fischer, M.J., Crommelin, D.J., 1993. The role of protein charge in protein-lipid interactions. pH-dependent changes of the electrophoretic mobility of liposomes through adsorption of water-soluble, globular proteins. Biochemistry 32, 4641–4649.

Binder, H., Zschornig, O., 2002. The effect of metal cations on the phase behavior and hydration characteristics of phospholipid membranes. Chem. Phys. Lipids 115, 39–61.

Cacace, M.G., Landau, E.M., Ramsden, J.J., 1997. The Hofmeister series: salt and solvent effects on interfacial phenomena. Q. Rev. Biophys. 30, 241–277.

Chen, T., 1992. Formulation concerns of protein drugs. Drug Dev. Ind. Pharm. 18, 1311–1354.

De Souza, N.C., Caetano, W., Itri, R., Rodrigues, C.A., Oliveira Jr., O.N., Giacometti, J.A., Ferreira, M., 2006. Interaction of small amounts of bovine serum albumin with phospholipid monolayers investigated by surface pressure and atomic force microscopy. J. Colloid Interf. Sci. 297, 546–553.

Dimitrova, M.N., Matsumura, H., Neitchev, V.Z., 1997. Kinetics of protein-induced flocculation of phosphatidylcholine liposomes. Langmuir 13, 6516–6523.

Fu, F.N., Fuller, M.P., Singh, B.R., 1993. Use of Fourier transform infrared/attenuated total reflectance spectroscopy for the study of surface adsorption of proteins. Appl. Spectrosc. 47, 98–102.

Green, R.J., Hopkinson, I., Jones, R.A.L., 1999. Unfolding and intermolecular association in globular proteins adsorbed at interfaces. Langmuir 15, 5102–5110.

Harrington, K.J., Syrigos, K.N., Vile, R.G., 2002. Liposomally targeted cytotoxic drugs for the treatment of cancer. J. Pharm. Pharmacol. 54, 1573–1600.

Hubner, W., Blume, A., 1998. Interactions at the lipid-water interface. Chem. Phys. Lipids 96, 99–123.

Kwon, K.O., Kim, M.J., Abe, M., Ishinomori, T., Ogino, K., 1994. Thermotropic behavior of a phospholipid bilayer interacting with metal ions. Langmuir 10, 1415–1420.

Leserman, L., 2004. Liposomes as protein carriers in immunology. J. Liposome Res. 14, 175–189.

Mantsch, H.H., McElhaney, R.N., 1991. Phospholipid phase transitions in model and biological membranes as studied by infrared spectroscopy. Chem. Phys. Lipids 57, 213–226.

McClellan, S.J., Franses, E.I., 2005. Adsorption of bovine serum albumin at solid/aqueous interfaces. Colloid. Surf. A 260, 265–275.

Mirabella, F.M., 1998. Attenuated total reflection spectroscopy. In: Mirabella, F.M. (Ed.), Attenuated Total Reflection Spectroscopy. John Wiley & Sons, New York, pp. 127–183.

Mollmann, S.H., Jorgensen, L., Bukrinsky, J.T., Elofsson, U., Norde, W., Frokjaer, S., 2006. Interfacial adsorption of insulin conformational changes and reversibility of adsorption. Eur. J. Pharm. Sci. 27, 194–204.

Norde, W., Giacomelli, C.E., 2000. BSA structural changes during homomolecular exchange between the adsorbed and the dissolved states. J. Biotechnol. 79, 259–268.

Oku, N., Yamazakia, Y., Matsuuraa, M., Sugiyamaa, M., Hasegawa, M., Nango, M., 2001. A novel non-viral gene transfer system, polycation liposomes. Adv. Drug Deliv. Rev. 52, 209–218.

Roberts, S.A., Kellaway, I.W., Taylor, K.M., Warburton, B., Peters, K., 2005. Combined surface pressure-interfacial shear rheology studies of the interaction of proteins with spread phospholipid monolayers at the air-water interface. Int. J. Pharm. 300, 48–55.

Sethuraman, A., Belfort, G., 2005. Protein structural perturbation and aggregation on homogeneous surfaces. Biophys. J. 88, 1322–1333.

Small, D.M., 1986. The Physical Chemistry of Lipids: From Alkanes to Phospholipids. Plenum Press, New York.

Tamm, L.K., Tatulian, S.A., 1997. Infrared spectroscopy of proteins and peptides in lipid bilayers. Q. Rev. Biophys. 30, 365–429.

Tang, J., Jiang, J., Song, Y., Peng, Z., Wu, Z., Dong, S., Wang, E., 2002. Conformation change of horseradish peroxidase in lipid membrane. Chem. Phys. Lipids 120, 119–129.

Tani, F., Murata, M., Higasa, T., Goto, M., Kitabatake, N., Doi, E., 1995. Molten globule state of protein molecules in heat-induced transparent food gels. J. Agric. Food Chem. 43, 2325–2331.

Vermette, P., Gauvreau, V., Pezolet, M., Laroche, G., 2003. Albumin and fibrinogen adsorption onto phosphatidylcholine monolayers investigated by Fourier transform infrared spectroscopy. Colloid. Surf. B 29, 285–295.

Wang, W., 1999. Instability, stabilization, and formulation of liquid protein pharmaceuticals. Int. J. Pharm. 185, 129–188.